

Regulation Performance of Regulatable Dry Gas Seal

SHUANGXI LI, QIAOFENG ZHU, JINING CAI, QIUXIANG ZHANG, ZHAOXU JIN

Colleague of Mechanical and Engineering

Beijing University of Chemical Technology

No.15 of North Three-ring East Road, Chao Yang District, Beijing

CHINA

buctlsx@163.com

Abstract—It is important for the regulatory efficiency and the popularization of R-DGS to study on the regulation performance of a Regulatable Dry Gas Seal (R-DGS). Based on gas lubrication theory, a numerical model for R-DGS was set up, the Steady Reynold equation and Disturbance Reynold equation were resolved by using finite element method to obtain the equilibrium film thickness, leakage rate and dynamic parameters. The universal law of the seal parameters was obtained under difference regulation ratio I and shaft speed. The running regulation test is processed and the regulation reliability of R-DGS with outer regulative gas source is proved. The results show that the sealing performance of R-DGS changes obviously with the regulation ratio (I); and the shaft speed also effect the sealing performance when the regulation ratio is $I < 1.5$. Comprehensive regulation performance of Pi-DGS is better than Po-DGS. The research results verify the feasibility of R-DGS and provide a reference for user to design and regulatory the R-DGS.

Keywords:-Regulatable dry gas seal; Regulation performance; Steady state; Disturbed State.

1 Introduction

Dry Gas Seal (DGS), in particular, is widely applied in medium and high speed rotating machinery in recent years due to its advantages in low wear, long lifespan and low energy consumption [1]. The special lift geometries, such as spiral grooves or circumferential waviness fabricated on the seal faces have proven to be effective to improve the tribological performance of the slider.

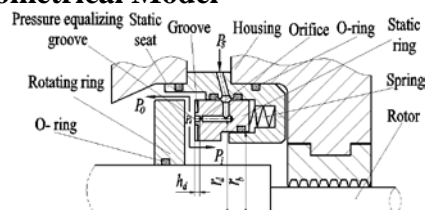
However, the application of DGS on low-speed and unsteadiness occasions is limited, because the hydrodynamic effect may not be strong enough for the seal in use and its low stability and reliability should be improved further. In order to solve the problem, the Regulatable Dry Gas Seal (R-DGS) has been invented, which is making use of the hydrodynamic effect and the hydrostatic effect to keep a reasonable sealing clearance between seal faces [2]. R-DGS is exceedingly applicable to aviation, aerospace and military domain benefited from its adaptation in high-low speed and active regulation performance.

Up to now, several relevant researches of the seal holding potential for online regulation have been published. Woff et al [3] and Zou et al [4] researched respectively the controllable capability of the noncontacting mechanical seal and realized the goal of adjusting the equilibrium film thickness online. And then, Zou et al [5] confirmed the feasibility of turning the contacting mechanical seal into

noncontacting status by flexible installment. Aiming at the sealing clearance, Zhang et al [6] introduced a new kind of controllability noncontacting seal, which is taking advantages of electromagnetic device. Zhu et al [7] analyzed the initiative adjustment performance of hydrostatic dry gas seal and confirmed it through experiments. However, most of the theoretical researches about the seal capability were gained with specific gas film thickness under a certain conditions. Then the evolution of seal capability as the film thickness is analyzed. In fact, the film thickness is changing along with working conditions, and the relevant performances are also unstable. Therefore, by solving the Reynolds equation and the axial force balance equation simultaneously in this paper, and studied the effect of the regulation ratio (I) and the shaft speed on the regulation performance of R-DGS through, then confirmed later through experiments.

2 Analytical Models

2.1 Geometrical Model



(a) The working principle of R-DGS

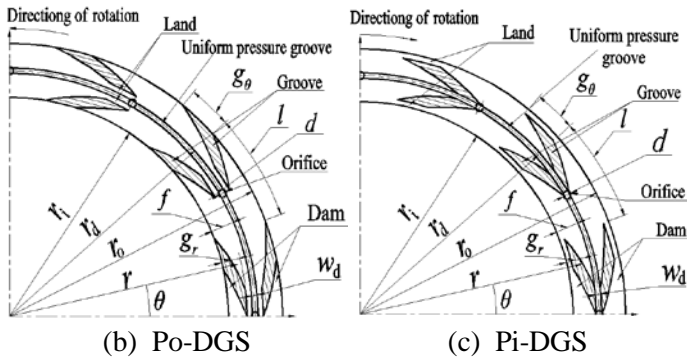


Fig.1. Principle and grooved faces of R-DGS

The principle of R-DGS is shown in Fig.1, the inside radius, the outside radius and the balance radius of the seal face are set as r_i , r_o and r_b . The rotor rotates along with the shaft, while the stator is mounted on stator base, O-ring is the secondly seal, and springs provide the closing force. The stator was processed with the uniform pressure groove and the spiral groove on its seal face, the uniform pressure groove is connect with the throttling structure, external regulative gas (Pressure P_s) flows through the throttling structure into the sealing clearance (Pressure drop P_d) and produces opening force for the hydrostatic effect, and the opening force will be raised further when the rotor is rotating [2]. It must be mentioned here that, by adjusting the pressure of regulative gas, the equilibrium film thickness and leakage can be changed regularly, thereby the purpose of adjusting the seal performances of R-DGS will also be realized.

The grooved seal face configuration studied in this paper is also illustrated in Fig.1. According to the function of grooves, R-DGS could be classified as the Pumping-in Dry Gas Seal (Pi-DGS) and the Pumping-out Dry Gas Seal (Po-DGS) [2]. The spiral-groove is adopted in this paper as well as the throttle orifice due to their superior performance and easy machining. The main geometric parameters of and working conditions are shown in Table 1.

Table.1 Parameters of the model

| Sturcture Parameter | Value |
|--|-------|
| Inside radius of gas film r_i /mm | 81 |
| Outside radius of gas film r_o /mm | 101 |
| Balance radius r_b /mm | 86 |
| Throttle orifice diameter d /mm | 0.2 |
| Number of throttle orifices N_o | 12 |
| Radial position of orifice and uniform pressure groove r_d /mm | 91 |
| Uniform pressure groove depth h_d /mm | 0.2 |
| Uniform pressure groove width w_d /mm | 0.4 |
| Land-to-groove ratio $\gamma=g_\theta/(g_\theta+l)$ | 0.5 |
| Seal groove ratio $\delta=g_r/f$ | 0.7 |

| Spiral groove angle α° | 20 |
|--|---------|
| Number of spiral grooves N_g | 12 |
| Spiral groove depth h_g /mm | 0.006 |
| Operating Parameter | |
| Pressure at the inner radius(p_{abs}) p_i /MPa | 0.1 |
| Pressure at the outer radius(p_{abs}) p_o /MPa | 0.2-0.6 |
| Pressure of regulative gas(p_{abs}) p_s /MPa | 0.3-0.9 |
| Shaft speed $n/\times 10^3$ rpm | 2-5 |
| Spring force f_s /N | 60 |

2.2 Mathematical model of Steady State

The R-DGS configuration is axial force balanced in the steady state. Generally, the unfixed ring that could be compensatory axially, the stator in the following, is chosen to be the object of study for the mechanical equilibrium.

The closing force of the stator f_c can be obtained as follows.

$$f_c = \pi(r_o^2 - r_b^2)(p_i - p_o) + \pi(r_o^2 - r_b^2)p_i + f_s \quad (1)$$

The opening force of the stator f_o can be obtained in the following.

$$f_o = \int_0^{2\pi} \int_{r_i}^{r_o} p r dr d\theta \quad (2)$$

where r and θ present the cylindrical coordinates, p presents the film pressure.

Thus, the following equation is acquired according to axial force balance.

$$f_c = f_o \quad (3)$$

The gas film between the seal is assumed to be constant and laminar. The velocity and pressure gradient along with the film thickness are neglected. For the ideal gas, the gas film pressure is obtained by solving the Reynolds equation (4) [8].

$$\frac{\partial}{r^2 \partial \theta} \left(\frac{\rho h^3}{\eta} \frac{\partial p_0}{\partial \theta} \right) + \frac{\partial}{r \partial r} \left(\frac{r \rho h^3}{\eta} \frac{\partial p_0}{\partial r} \right) + 12 \rho \tilde{\nu} \delta_j = 6\omega \frac{\partial(\rho h)}{\partial \theta} \quad (4)$$

Where h describes the film thickness; η is the dynamic viscosity; ρ is the density; $\rho \tilde{\nu}$ is the mass flow rate through unit cross-sectional area of the orifice; δ_j is the Kronecker number.

As mentioned above, the Reynolds equation provides the film pressure distribution p_0 numerically, that induce the solution of opening force f_o , but at the same time the f_o is restricted by axial force balance, as demonstrated in Eq.(3). Hence, there is tight coupling between Eq.(3) and Eq.(4). For dealing with the situation, the film thickness should be evaluated variably until the opening force f_o acquired from

Eq.(2) and Eq.(4) is equal to f_c and then the h_o now is considered as the accurate actual working performance, as illustrated in literature [9].

Therefore, considering the mandatory boundary conditions and the periodic boundary conditions as emphasized by Liu, et al [8], all of the performance parameters could be acquired based on the equilibrium film thickness h_o .

2.3 Mathematical model of Dynamic Static

Study on dynamic performance of R-DGS contains dynamic stiffness and damping coefficients. And perturbation pressure can be express as follows.

$$p' = (p_{zr} + ip_{zi})z + (p_{ar} + ip_{ai})\alpha + (p_{\beta r} + ip_{\beta i})\beta \quad (5)$$

Dynamic stiffness and damping coefficients be express as follows.

$$\begin{cases} \begin{bmatrix} K_{zz} & K_{zx} & K_{zy} \\ K_{xz} & K_{xx} & K_{xy} \\ K_{yz} & K_{yx} & K_{yy} \end{bmatrix} = \begin{bmatrix} -\frac{\partial F_z}{\partial z} & -\frac{\partial F_z}{\partial \alpha} & -\frac{\partial F_z}{\partial \beta} \\ -\frac{\partial M_x}{\partial z} & -\frac{\partial M_x}{\partial \alpha} & -\frac{\partial M_x}{\partial \beta} \\ -\frac{\partial M_y}{\partial z} & -\frac{\partial M_y}{\partial \alpha} & -\frac{\partial M_y}{\partial \beta} \end{bmatrix} \\ \begin{bmatrix} C_{zz} & C_{zx} & C_{zy} \\ C_{xz} & C_{xx} & C_{xy} \\ C_{yz} & C_{yx} & C_{yy} \end{bmatrix} = \begin{bmatrix} -\frac{\partial F_z}{\partial \dot{z}} & -\frac{\partial F_z}{\partial \dot{\alpha}} & -\frac{\partial F_z}{\partial \dot{\beta}} \\ -\frac{\partial M_x}{\partial \dot{z}} & -\frac{\partial M_x}{\partial \dot{\alpha}} & -\frac{\partial M_x}{\partial \dot{\beta}} \\ -\frac{\partial M_y}{\partial \dot{z}} & -\frac{\partial M_y}{\partial \dot{\alpha}} & -\frac{\partial M_y}{\partial \dot{\beta}} \end{bmatrix} \end{cases} \quad (6)$$

Disturbance momentum of turning moment F_z' , M_x' , and M_y' is the integral of p' .

$$\begin{cases} F_z' \\ M_x' \\ M_y' \end{cases} = \iint_{\Omega} \begin{bmatrix} p' \\ p' r \sin \theta \\ -p' r \cos \theta \end{bmatrix} d\Omega \quad (7)$$

The expressions of dynamic stiffness and damping coefficients can be obtained by solving Eq. (5), Eq. (6) and Eq. (7), which contain the perturbation pressure ($p_{zr}, p_{zi}, p_{ar}, p_{ai}, p_{\beta r}, p_{\beta i}$).

The transient film pressure distribution can be obtained by solving the Reynolds equation (8).

$$\begin{aligned} & \frac{\partial}{r^2 \partial \theta} \left(\frac{\rho h^3}{\eta} \frac{\partial p}{\partial \theta} \right) + \frac{\partial}{r \partial r} \left(\frac{r \rho h^3}{\eta} \frac{\partial p}{\partial r} \right) + 12 \rho \tilde{v} \delta_j \\ & = 6\omega \frac{\partial(\rho h)}{\partial \theta} + 12 \frac{\partial(\rho h)}{\partial t} \end{aligned} \quad (8)$$

Using the perturbation method the Steady Reynold equation and Disturbance Reynold equation can be separated from Eq.(8), and considering the mandatory boundary conditions as illustrated in literature [2], then the computed result of the perturbation pressure ($p_{zr}, p_{zi}, p_{ar}, p_{ai}, p_{\beta r}, p_{\beta i}$) can be used for solving the values of dynamic stiffness and damping coefficients.

3 Results and Discussion

In order to expand the application of the researches, the regulation ratio Γ is introduced to stands for the change of regulative gas pressure.

$$\Gamma p = (P - p) / p_i \quad (9)$$

3.1 Effect of Regulation Ratio

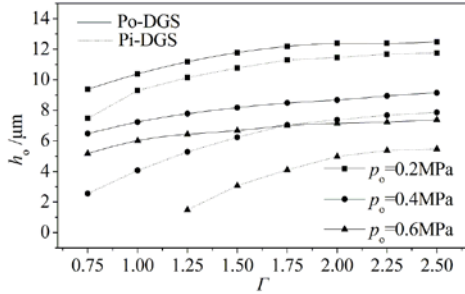
The evolution of sealing performance as the regulation ratio under different working pressure is shown in Fig.2. As the Fig.2.(a), (b), it can be seen that the equilibrium film thickness greatly increases with the increase of the regulation ratio Γ when $\Gamma < 2$, while the equilibrium film thickness changes little when the regulation ratio is $\Gamma > 2$. In other words, for the R-DGS with certain structure parameters, the equilibrium film thickness increases obviously with increasing regulative gas pressure. In addition, the inward leakage rate (q_i) and outward leakage rate (q_o) have the same trend as h_o with the increasing regulation ratio, but when $\Gamma > 2$, the leakage rate are also changes obviously.

Three working pressure cases, 0.2MPa, 0.4MPa and 0.6MPa are presented in Fig.2 (a) and (b). Both the equilibrium film thickness and leakage rate changes with the increase of the working pressure. In the case of $\Gamma=2$, when the working pressure increase from 0.2MPa to 0.4MPa, the equilibrium film thickness of Pi-DGS decreases 35.6% and the Po-DGS decreases 29.9%, while the increase of inward leakage rate of Pi-DGS is 30.7% and the Po-DGS is 27.4%. The change of the equilibrium film thickness is larger than that of the leakage rate.

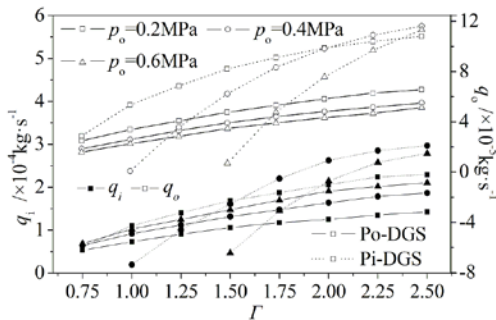
The evolution of dynamic performance parameters of the R-DGS as the regulation ratio under different working pressure is shown in Fig.2 (c), (d) and (e). It can be seen that k_{zz} increases with the increase of the regulation ratio Γ but c_{zz} decreases. Variation of radial film parameters similar to the axial film parameters, but the variation of angular film parameters is opposite. $k_{xy}(k_{yx})$ decreases and $c_{xy}(-c_{yx})$ increases with the increase of the regulation ratio Γ . The regulation ratio Γ has the significant effect on the axial film parameters and has little effect on the

radial film parameters and angular film parameters for the R-DGS.

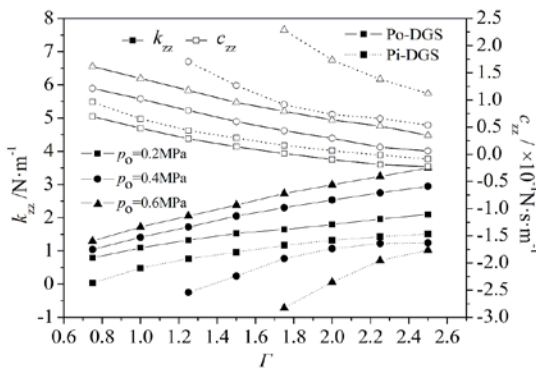
The parameters of Pi-DGS have larger parameter changes per unit pressure changes. Another important result is that the change of sealing performance of Pi-DGS along with the regulation ratio Γ is greater than Po-DGS. It means that the regulation performance of Pi-DGS is better than Po-DGS.



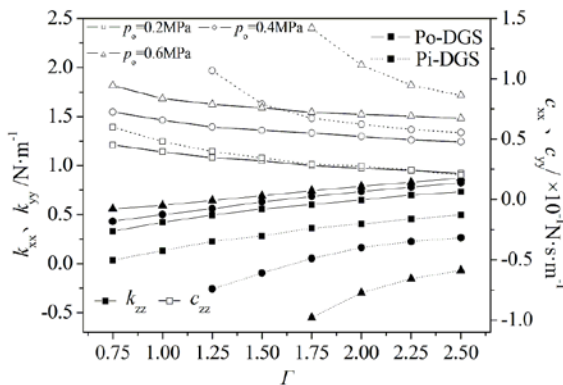
(a) h_0 vs Γ



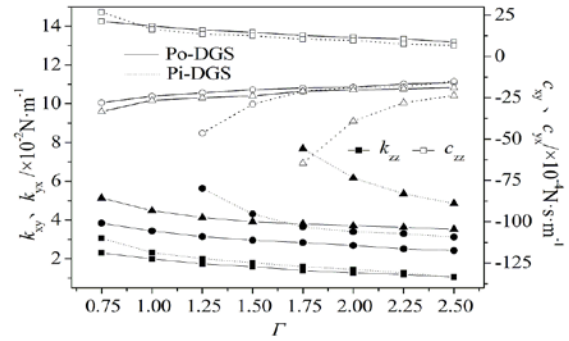
(b) q_i, q_o vs Γ



(c) k_{zz}, c_{zz} vs Γ



(d) $k_{xx}, k_{yy}, c_{xx}, c_{yy}$ vs Γ



(e) $k_{xy}, k_{yx}, c_{xy}, c_{yx}$ vs Γ

Fig.2 Sealing performance of R-DGS with different regulation ratio Γ under different working pressure ($n=2500$ r/min)

The regulation reliability of R-DGS is confirmed by the variation of sealing performance along with the regulation ratio Γ . However, in view of measurement accuracy and promptness, the equilibrium film thickness is adopted to be the target to regulate the R-DGS online. In the actual working process, the preferred equilibrium film thickness under different working pressures are listed in Table.2.

Table 2 Preferred Values of Equilibrium Film Thickness

| $P_o/0.1$ MPa | 2~3 | 3~5 | 5~8 | 8~10 |
|------------------|-----|-----|-----|------|
| Po-DGS / μ m | 11 | 7 | 5 | 4 |
| Pi-DGS / μ m | 10 | 6 | 4 | 4 |

3.2 Effect of Shaft Speed

Fig.3 demonstrates the evolution of sealing performance as the regulation ratio under different shaft speed (n), when the working pressure is $p_o=0.4$ MPa. It is clearly shown that the behaviours of the curves in Fig.3 are similar to that in Fig.2. However, the sealing performance of R-DGS changes obviously with the increase of the shaft speed when the regulation ratio is $\Gamma < 1.5$, while the change can be neglected when the regulation ratio is $\Gamma > 1.5$. A possible reason for the phenomenon could be attributed to thickness change of gas film, which results in great effect on the hydrodynamic effect and hydrostatic effect.

As the research method proposed above, the preferred equilibrium film thickness under different shaft speeds are listed in Table.3.

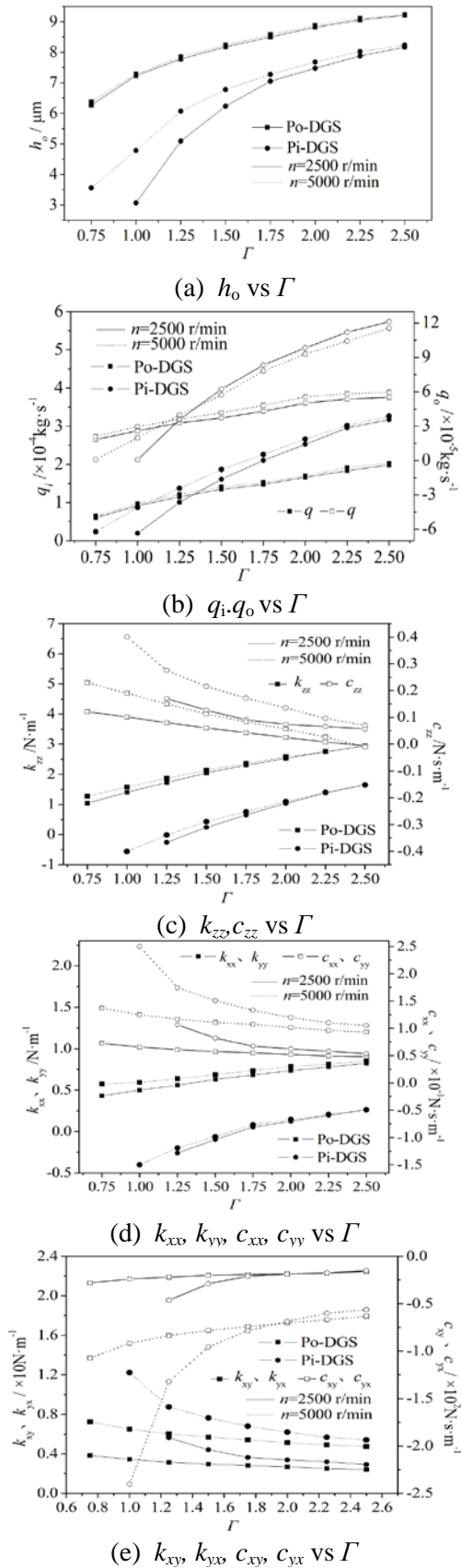


Fig.3 Sealing performance of R-DGS with different regulation ratio Γ under different shaft speed ($P_o=0.4MPa$)

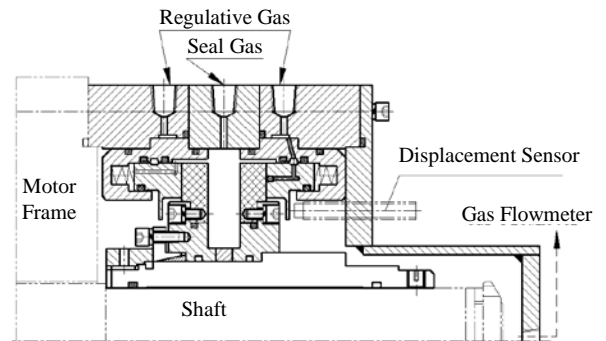
Table 3 Preferred Values of Equilibrium Film Thickness

| $n / 1000rpm$ | 2~4 | 4~6 | 6~8 | 8~10 |
|------------------|-----|-----|-----|------|
| Po-DGS / μm | 8 | 8 | 9 | 9 |
| Pi-DGS / μm | 6 | 7 | 7 | 8 |

4 Experimental Verification

In order to verify the reliability of the regulation performance researched in this paper, the R-DGS have been designed and manufactured. The structure parameters are in agreement with Table 1 and the working pressure and shaft speed are respectively $p_o=0.4MPa$ and $n=2500rpm$, and it is shown in Fig. 4.

A comparison between the theoretical values and the experimental values of the sealing performance including the equilibrium film thickness h_o and the inward leakage q_i is shown in Fig.5. It is worth mentioning here that the equilibrium film thickness h_o is measured axially by use of eddy current sensor named Bently 3300 and the inward leakage q_i is acquired with the help of gas flowmeter named Honeywell 720P1. The h_o and q_i are the significant indexes to evaluate the sealing performance of R-DGS, which can predict the state of the seal to some extent.



(a) Experimental installation of R-DGS



(b) Physical map of R-DGS

Fig.4 Experimental installation and Physical map of R-DGS

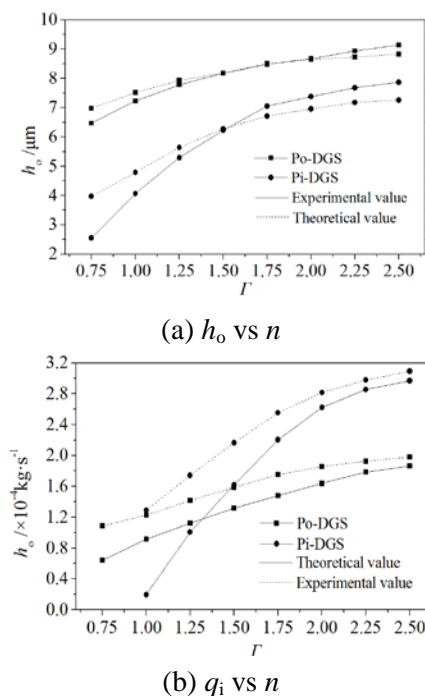


Fig.5 Experimental verification

From Fig.5 it appears very clearly that with the experimental values the equilibrium film thickness h_0 is larger than with the theoretical values along with the augment of regulation ratio, as well as the inward leakage q_i . Furthermore, as Γ increases, the difference increases. The reasons are in the following: as a result of manufacture-errors, fix-errors and so on, it appears that the seal faces is rough and the stator is deflected, and then, the additional dynamic effect strengthens the opening force, thereby enhancing the values of h_0 and q_i . However, when the proposed practical factors are considered, the theoretical values of h_0 and q_i agree well with the experimental ones, otherwise, the analysis results illustrated above are credible.

5 Conclusions

The regulation ratio and the shaft speed was obtained by solving the Steady Reynold equation and Disturbance Reynold equation, then the effect of them was studied, the regulation reliability of R-DGS is confirmed, and a series of preferred values of the equilibrium film thickness was obtained under difference regulation ratio and shaft speed. The following conclusions can be obtained from the result discussion above:

(1) The sealing performance parameters of R-DGS changes obviously with the regulation ratio Γ change, while the regulation ratio is maintained at low value ($\Gamma < 2$), and the leakage rate still increase with the increase of the regulation ratio, so the regulation ratio should be controlled in low value.

(2) Shaft speed have significant effect on the most of sealing performance parameters of R-DGS while the regulation ratio is maintained at low value ($\Gamma < 1.5$) except the leakage rate.

(3) The sealing performance parameters of R-DGS changes obviously with the regulation ratio while the low speed.

(4) The regulation performance of Pi-DGS is better than the regulation performance of Po-DGS.

Because the lack of the length of the article, more kinds of the structure and operate parameters should be studied in the future, and the thermal and elastic deformations should be considered.

Acknowledgment

This work was supported by the National Basic Research Program of China (973) (Grant No. 2012CB026000).

References

- [1] Faria M.T.C, An efficient finite element procedure for analysis of high-speed spiral groove gas faced seals. *ASME J. of Tribology*, 2001, 123(1): 205-210.
- [2] Li shuangxi, Zhang shuqiang, Cai ji'ning, Zhang qiuxiang. Performance study of dynamic — hydrostatic hybrid gas seal. *Tribology*, 2011, 05: 457-466. (in Chinese)
- [3] Woff P, Salant R.F. Electronically controlled mechanical seal for aerospace applications: Part II transient tests. *Stle Stribology Transactions*. 1995, 38(1): 51-56.
- [4] Zou M, Dayan J, Green I. Dynamic simulation and monitoring of a non-contacting flexibly mounted rotor mechanical face seal. *Proceedings of the Institution of Mechanical Engineers: Part C Journal of Mechanical Engineering Science*. 2000, 214(9): 1195-1206.
- [5] Zou M, Dayan J, Green I. Feasibility of contact elimination of a mechanical face seal through clearance adjustment. *Proceedings of the Institution of Mechanical Engineers: Part C Journal of Mechanical Engineering Science*. 2000, 214(9): 1195-1206.
- [6] Zhang guoyuan, Zhao weigang, Chen yao, Wei junchao. Active controllability and separation mechanics of non-contact hydrostatic mechanical seal. *Journal of Aerospace Power*, 2014, 29(10): 2516-2522. (in Chinese)
- [7] Zhu liang, Li shuangxi, Zhang qiuxiang, Cai ji'ning. Experiment study on active control of non-contacting mechanical seal. *Fluid Machinery*, 2012, 40(7): 1-6. (in Chinese)

- [8] Liu tun, Liu yuhua, Chen shijie. *Aerostatic gas lubrication*. Harbin: Harbin Institute of Technology Press, 1990. (in Chinese)
- [9] Cheng xiangping, Peng xudong, Meng xiangkai. Analysis of sealing performance of sealing end face with diamond pores,” *Journal of Shanghai Jiaotong University*, 2014. 48(1): 33-38. (in Chinese)